Rabi Oscillations and Excitation Trapping in the Coherent Excitation of a Mesoscopic Frozen Rydberg Gas

M. Reetz-Lamour, T. Amthor, J. Deiglmayr, and M. Weidemüller*

Physikalisches Institut der Universität Freiburg, Hermann-Herder-Strasse 3, D-79104 Freiburg, Germany

(Received 13 November 2007; published 26 June 2008)

We demonstrate the coherent excitation of a mesoscopic ensemble of about 100 ultracold atoms to Rydberg states by driving Rabi oscillations from the atomic ground state. We employ a dedicated beam shaping and optical pumping scheme to compensate for the small transition matrix element. We study the excitation in a weakly interacting regime and in the regime of strong interactions. When increasing the interaction strength by pair state resonances, we observe an increased excitation rate through coupling to high angular momentum states. This effect is in contrast to the proposed and previously observed interaction-induced suppression of excitation, the so-called dipole blockade.

DOI: 10.1103/PhysRevLett.100.253001 PACS numbers: 32.80.Rm, 03.65.Yz, 34.20.Cf

Rydberg atoms, with their rich internal structure, have been in the focus of atomic physics for more than a century [1]. In the past decade, Rydberg physics was extended to laser-cooled atomic gases which allowed the study of a frozen system with controllable, strong interactions and negligible thermal contributions. This has opened a wide field in both experiment and theory covering such diverse areas as resonant energy transfer [2,3], plasma formation [4,5], exotic molecules [6,7], and quantum random walks [8,9]. In addition, these frozen Rydberg systems have been proposed as a possible candidate for quantum information processing [10,11]. However, the coherent excitation of Rydberg atoms, an important prerequisite for quantum information protocols, has proven a challenging task. While Rabi oscillations between different Rydberg states have been demonstrated and thoroughly analyzed before [12], Rabi oscillations between the ground state and Rydberg states of atoms have not been observed directly so far, mainly owing to the small transition matrix element.

In this Letter, we report on the experimental realization and observation of Rabi oscillations between the ground and Rydberg states of ultracold atoms. We demonstrate how strong interatomic interactions influence the coherent excitation of a mesoscopic cloud of atoms. We show that an interaction-induced coupling to a larger number of internal states can be used to trap the excitation. Employed in a controlled way, this effect offers future applications in the experimental realization of quantum random walks with exciton trapping [9].

Our experiments are performed with a magneto-optical trap (MOT) of about 10^7 ^{87}Rb atoms at densities of 10^{10} cm^{-3} and temperatures below 100 μK. Rydberg excitation is achieved with two counterpropagating laser beams at 780 and 480 nm (see Fig. 1). The laser at 780 nm is collimated to a waist of 1.1 mm ensuring a constant Rabi frequency of $2\pi \times 55$ MHz over the excitation volume as determined from Autler-Townes splittings [13]. The laser at 480 nm (typical power 40 mW) is referenced to a temperature-stabilized ZERODUR resonator. Its beam is shaped with a diffractive optical element that produces a flattop beam profile, characterized with a CCD camera (spatial resolution 5.6 μm) [14]. The measured flattop is depicted in Fig. 1(b). This setup allows a tightly focused beam with high intensity and at the same time overcomes the limits of a Gaussian beam shape. Gaussian beams have been used for stimulated adiabatic passage to high Rydberg states [13,15] but do not allow the observation of synchronous Rabi floppings in a mesoscopic sample due to the wide range of intensities across the beam [13]. In order to address only atoms in the flattop region, we use spatially selective optical pumping (see Fig. 1): The magnetic field of the MOT is turned off 3 ms before excitation [16]. After turning off the trapping lasers, all atoms are pumped to the $F = 1$ hyperfine component of the $5S_{1/2}$ ground state within 300 μs. A small tube of atoms perpendicular to the excitation beams is transferred to the $F = 2$ hyperfine component with a 1 μs pulse of a tightly

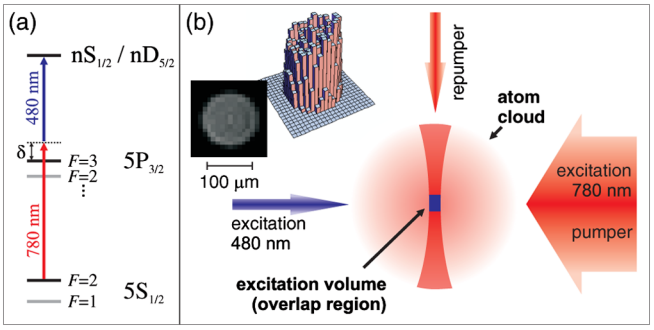

FIG. 1 (color online). (a) Relevant level scheme for two-photon excitation of rubidium. (b) Preparation of a mesoscopic subensemble. All atoms are pumped to the $F = 1$ hyperfine component of the ground state. Only a tight tube of atoms is pumped to $F = 2$ whence the excitation originates. Within this tube, a mesoscopic subensemble containing about 100 atoms is excited to Rydberg states with two counterpropagating laser beams at 780 and 480 nm. The latter has a flattop intensity profile shown in the inset, to ensure a constant Rabi frequency.

focused repumping beam (waist 10 μm, 10 nW). Only these atoms are resonant with the excitation lasers. They are optically pumped to the stretched $F = 2, m_F = 2$ state by a 1 μs pulse of a σ^+-polarized pumper beam superimposed with the excitation lasers. From this state we can excite both stretched nS and nD states depending on the helicity of the excitation laser polarization; n denotes the principal quantum number. By maintaining the two-photon resonance but detuning from the intermediate state $5P_{3/2}$ by typically $\delta/2\pi = 140$ MHz, this state experiences negligible population and atoms are directly transferred to the Rydberg state [13]. The overlap between the repumping laser and the 480 nm laser defines the excitation volume of about $10\ \mu\text{m} \times 10\ \mu\text{m} \times 100\ \mu\text{m}$, corresponding to $\sim$100 atoms [see Fig. 1(b)]. Rydberg atoms are detected by field ionization and accelerated onto a microchannel plate detector. There is no signal for electric fields below the ionization threshold; therefore, we can rule out the presence of spurious ions during excitation. After detection, the MOT is turned back on, and the whole cycle is repeated every 70 ms. Our setup allows us to compensate electric fields $\mathcal{E}_\perp$ in a direction perpendicular to the excitation lasers. Field components parallel to the field plates cannot be compensated and are determined from Stark shifts to be $\mathcal{E}_\parallel = 160$ mV/cm [17]. The field values given in the text represent the total field $\mathcal{E} = (\mathcal{E}_\parallel^2 + \mathcal{E}_\perp^2)^{1/2}$.

Figure 2 shows the measured fraction of excited Rydberg atoms in the $31D_{5/2}$ state as a function of excitation time. Rabi oscillations are clearly visible. We observe the same temporal dependence for both nS and nD states with $n < 40$ at both low and high atom densities. This indicates that for these small n values the observed Rabi oscillations are not affected by Rydberg-Rydberg interactions and that all atoms perform identical Rabi oscillations simultaneously. The solid line in Fig. 2 is a theoretical prediction with a blue Rabi frequency of $2\pi \times 27$ MHz which takes the measured time dependence of the excitation pulses into account. It incorporates three sources of dephasing: the remaining admixture of the intermediate state, the residual intensity distribution of the flat-top beam profile, and a finite laser bandwidth of 2.4 MHz. With increasing importance, these three sources lead to the observed damping of the measured Rabi oscillations. A detailed discussion together with quantitative comparisons between measured and calculated Rabi frequencies and other systematic verifications has been published in Ref. [14]. For longer times ($\gtrsim$200 ns), the excitation probability reaches a steady state value of 0.5. This value is used to calibrate the detector signal [18].

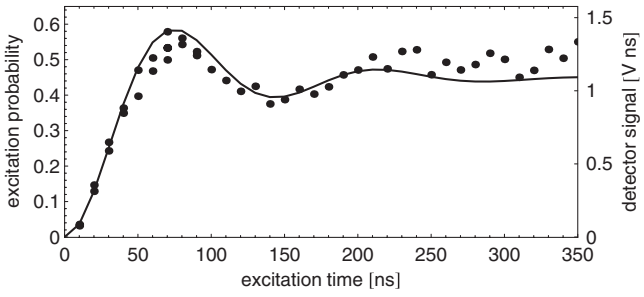

FIG. 2. Rabi oscillations between the $5S_{1/2}$ and $31D_{5/2}$ states of ^{87}Rb. Each dot is an average of measurements over 28 experimental repetition cycles. The solid line shows the simulated excitation probability taking the measured intensity distribution, the residual $5P_{3/2}$ admixture, and our finite laser linewidth into account. The scaling between the detector signal and simulated excitation probability is a free parameter that represents the detector efficiency.

The observation of Rabi oscillations between ground and Rydberg states is a first step towards the implementation of quantum information protocols with cold Rydberg gases. The most promising protocols further rely on the so-called dipole blockade [10,11]. The dipole blockade describes a system in which the excitation of more than one atom is inhibited due to interaction-induced energy shifts. It allows one to store a single excitation in a mesoscopic cloud of atoms and is accompanied by an increased collective Rabi frequency, evidence of which was observed only recently [19]. The first experimental signatures of the blockade were observed as a suppression of excitation [20,21] due to the extraordinarily strong van der Waals interactions at large values n. Recently, a similar effect was observed at lower values of n by using pair state resonances to switch from van der Waals to the stronger resonant dipole-dipole interaction with an external electric field [22].

For rubidium, nD states offer similar resonances. Figure 3 shows the electric field dependence of the in-

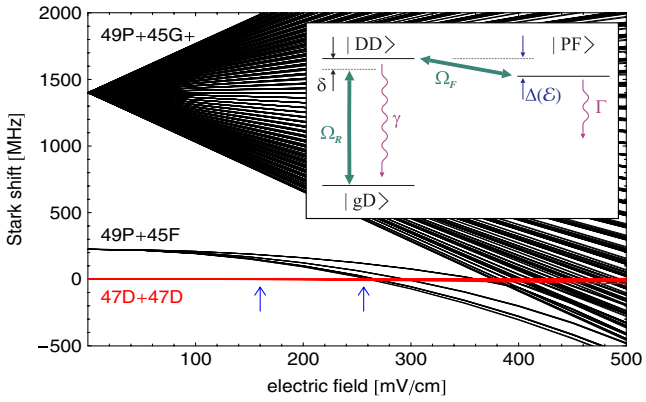

FIG. 3 (color online). Stark shift of dipole-coupled pair states around the $47D_{5/2} + 47D_{5/2}$ asymptote. The two arrows mark the total electric field at which the two spectra of Fig. 5 are taken. The inset shows a simplified level scheme for this system involving the coherent excitation of an atom pair from $|gD\rangle$ to $|DD\rangle$ with a Rabi frequency Ω_R, a laser detuning δ, and an effective linewidth γ. $|DD\rangle$ is dipole coupled to an almost degenerate pair $|PF\rangle$ with an interaction energy $\hbar\Omega_F$ and a field-dependent energy difference $\hbar\Delta(\mathcal{E})$. The dephasing of the dipole coupling is phenomenologically described by a decay rate Γ (see text).

volved pair states. At vanishing electric field, two $47D_{5/2}$ atoms experience van der Waals interaction. At an electric field of $\sim$260 mV/cm, the $47D_{5/2} - 47D_{5/2}$ pair state becomes energetically degenerate with the dipole-coupled $49P_{3/2} - 45F_J$ ($J = 5/2, 7/2$) pair state. This changes the interaction to long-range resonant dipole interaction. In contrast to the picture of the dipole blockade, however, the increased interaction strength does not translate into a reduced excitation probability at the atomic resonance: Figure 4 shows the temporal evolution of the $47D_{5/2}$ population for two different densities. For the lower density of 4.7×10^9 cm^{-3} (gray points), we observe damped Rabi floppings similar to low-n states. For the higher density (10^{10} cm^{-3}, black points), we observe an increased excitation that clearly exceeds 0.5. This means that part of the atoms accumulate in Rydberg states which are not coupled to the ground state by the laser field. The effect is clearly density-dependent and must therefore be interaction-induced.

We can heuristically reproduce the observations with an analytical model illustrated in Fig. 3. It incorporates the coherent excitation of a pair $|gD\rangle$ of a ground state atom $|g\rangle$ and a $47D$ atom $|D\rangle$ to a pair $|DD\rangle$ of two $47D$ atoms as well as the coupling to the $|PF\rangle$ state with a field-dependent energy shift relative to $|DD\rangle$. We introduce a dephasing by a decay rate Γ from the $|PF\rangle$ state out of the three-level system. This system is an analog of the excitation of an optical three-level system and can be fully described by the according optical Bloch equations [23]. When only coherent couplings are considered ($\Gamma = 0$), the system exhibits the dipole blockade, and the excitation probability is reduced when increasing the density [24].

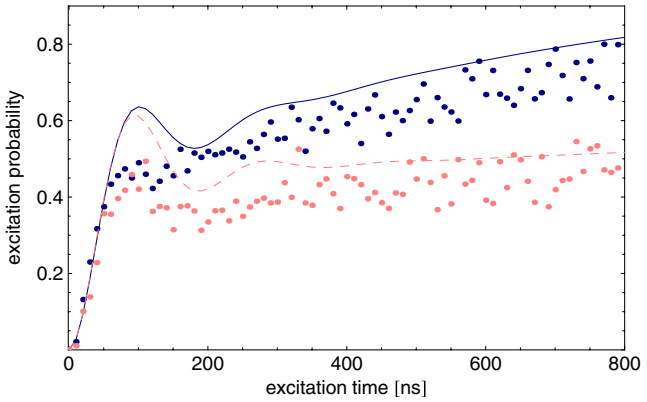

FIG. 4 (color online). Temporal evolution of the excitation probability for the $47D_{5/2}$ state at an electric field $\mathcal{E} = 160$ mV. For the smaller density of 4.7×10^9 cm^{-3} (gray dots), we see a damped Rabi oscillation similar to Fig. 2. For the higher density of 10^{10} cm^{-3} (black dots), the stimulated emission is suppressed leading to a constantly increasing Rydberg population. The lines are the solution of the model schematically shown in Fig. 3 for weak (dashed line) and strong (solid line) interactions. The excitation probability is derived from the detector signal with the scaling factor determined for Fig. 2 [18].

This is the case discussed in Ref. [22], where a resonance between well-defined pair states [$nP_{3/2} - nP_{3/2}$ and $nS_{1/2} - (n+1)S_{1/2}$ with $|m| = 1/2$] is used to suppress the Rydberg excitation. When including an additional incoherent coupling ($\Gamma > 0$), the behavior of the system changes drastically. Instead of an excitation suppression, the model now predicts an increased excitation as shown in Fig. 4.

The nature of such an incoherent coupling can be explained in the following way: In contrast to the well-defined pair states of the system in Ref. [22], the $45F_J$ state involved in our system is highly degenerate. As each substate has a different coupling strength, this leads to a dephasing. The residual electric field in our setup enhances this dephasing as it mixes different m_J levels and thus leads to a dipole coupling with all possible values of m_J, which involves 14 substates of the two values of $J = 5/2$ and $7/2$ for the $45F_J$ state and 6 substates for the $47D_{5/2}$ state. This dephasing suppresses the coupling back to $47D$ and accumulates atoms in $45F/49P$. Our detection cannot distinguish between $47D$, $49P$, and $45F$, and thus they all contribute to the excitation signal.

The solid line in Fig. 4 corresponds to model calculations with parameters for the excitation that are scaled from measured low-n Rabi oscillations. We have set Δ to the theoretical value $\Delta(\mathcal{E} = 160 \text{ mV}) = -2\pi \times 150$ MHz (see Fig. 3). This leaves two free parameters: The coupling strength $\Omega_F = 2\pi \times 40$ MHz and the dephasing rate $\Gamma = 2\pi \times 30$ MHz were chosen to achieve a good overlap with the experimental data. Both values are consistent with the theoretical value $\Omega_F^{\max} = 2\pi \times 64$ MHz for the strongest coupling between the stretched states ($m_J = J = \ell + 1/2$) at the most probable interatomic distance of 2.6 μm. The dashed line corresponds to a low-density model where Ω_F and Γ are scaled down proportional to the density (as expected for a $1/R^3$-dependent interaction).

With the same values for Ω_F and Γ, our model also explains spectral measurements shown in Fig. 5. By changing the electric field, we tune the energy difference between the $|DD\rangle$ and $|PF\rangle$ pair states. Figure 5(a) shows a measured spectrum of the $47D_{5/2}$ line at $\mathcal{E} = 160$ mV/cm ($\mathcal{E}_\perp = 0$) together with model calculations. All model parameters are the same as those for the excitation time scan in Fig. 4. Figure 5(b) shows a spectrum at $\mathcal{E} = 260$ mV/cm corresponding to $\Delta = 0$. The dashed line shows the model result in the low-density limit ($\Omega_F = 0$), and the solid line includes a coupling with $\Omega_F = 2\pi \times 5$ MHz and $\Gamma = 2\pi \times 30$ MHz, both chosen to yield the best overlap with the experiment. We attribute the reduced coupling strength Ω_F to the increased electric field which splits the involved states, effectively reducing Ω_F from 40 MHz at 160 mV to 5 MHz at 260 mV. There are three distinct features of the measured spectra at higher densities: line broadening, an enhanced excitation probability, and an electric field-dependent shift. The model qualitatively describes all of these features.

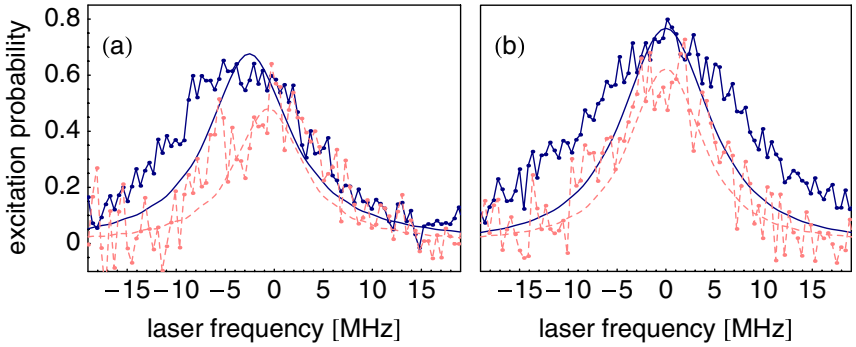

FIG. 5 (color online). (a) The $47D_{5/2}$ line at an electric field of $\mathcal{E} = 160$ mV/cm at densities of 10^{10} (solid blue line) and 4.7×10^9 cm^{-3} (dashed red line). For the higher density, we observe a line shift and broadening and an increased excitation probability. The smooth lines are the result of model calculations. The line shift is a result of an energy difference between $|DD\rangle$ and $|PF\rangle$. (b) The same for $\mathcal{E} = 260$ mV/cm. The line shift is reduced to zero, while broadening and increased excitation remain. All spectra are taken by scanning the 480 nm laser (fixed detuning from the intermediate level) with an excitation time of 400 ns.

We want to emphasize that the excitation trapping described here is not due to state redistribution by collisions with ions [25], since we have verified that there are no ions produced during the short excitation time. Furthermore, the excitation volume is too small to support avalanche ionization. The excitation enhancement is also different from the antiblockade for the case where the Autler-Townes splitting of the lower transition matches the Rydberg-Rydberg interaction energy [26]. The mechanism presented here can be seen as an energy diffusion *inside* the atom rather than a spatial diffusion which relies on internal state swapping *between* atoms and is the source of a different dephasing mechanism for energy transfer processes [2,3]. The internal energy dissipation can even counteract spatial diffusion by transferring the excitation into states with different angular momenta. This can result in pair states which are not *dipole*-coupled to other pair states, thus stopping spatial diffusion. This effect can be exploited as an exciton trap for continuous time quantum random walk experiments [9]. It also constitutes another constraint to states that are suited for dipole-blockade experiments besides the already identified zeros in Rydberg-Rydberg interactions for certain internal states [27] and atom pair alignments [28].

We thank T. Pohl for fruitful discussions and C. Pruss and W. Osten from the Institute for Technical Optics in Stuttgart for the production of the beam shaping element. The project is supported by the Landesstiftung Baden-Württemberg within the "Quantum Information Processing" program and by a grant from the Ministry of Science, Research and Arts of Baden-Württemberg No. (Az: 24-7532.23-11-11/1).

Note added.—After submission of this Letter, we became aware of a complementary work which demonstrates Rabi oscillation with an interaction-dependent damping in microscopic samples of 1–10 atoms [29].

*weidemueller@physik.uni-freiburg.de

[1] T. F. Gallagher, *Rydberg Atoms* (Cambridge University Press, Cambridge, England, 1994).
[2] W. R. Anderson, J. R. Veale, and T. F. Gallagher, Phys. Rev. Lett. **80**, 249 (1998).
[3] I. Mourachko *et al.*, Phys. Rev. Lett. **80**, 253 (1998).
[4] M. P. Robinson *et al.*, Phys. Rev. Lett. **85**, 4466 (2000).
[5] T. Amthor *et al.*, Phys. Rev. Lett. **98**, 023004 (2007).
[6] C. Boisseau, I. Simbotin, and R. Côté, Phys. Rev. Lett. **88**, 133004 (2002).
[7] C. H. Greene, A. S. Dickinson, and H. R. Sadeghpour, Phys. Rev. Lett. **85**, 2458 (2000).
[8] R. Côté *et al.*, New J. Phys. **8**, 156 (2006).
[9] O. Mülken *et al.*, Phys. Rev. Lett. **99**, 090601 (2007).
[10] D. Jaksch *et al.*, Phys. Rev. Lett. **85**, 2208 (2000).
[11] M. D. Lukin *et al.*, Phys. Rev. Lett. **87**, 037901 (2001).
[12] T. R. Gentile *et al.*, Phys. Rev. A **40**, 5103 (1989).
[13] J. Deiglmayr *et al.*, Opt. Commun. **264**, 293 (2006).
[14] M. Reetz-Lamour *et al.*, New J. Phys. **10**, 045026 (2008).
[15] T. Cubel *et al.*, Phys. Rev. A **72**, 023405 (2005).
[16] We use the thermal expansion of the cloud to change the ground state density by increasing this time up to 15 ms.
[17] K. Singer *et al.*, J. Phys. B **38**, S321 (2005).
[18] This scaling factor is inversely proportional to the number of atoms in the excitation volume and therefore to the density. Absolute densities are determined by absorption imaging.
[19] R. Heidemann *et al.*, Phys. Rev. Lett. **99**, 163601 (2007).
[20] D. Tong *et al.*, Phys. Rev. Lett. **93**, 063001 (2004).
[21] K. Singer *et al.*, Phys. Rev. Lett. **93**, 163001 (2004).
[22] T. Vogt *et al.*, Phys. Rev. Lett. **97**, 083003 (2006).
[23] R. M. Whitley and C. R. Stroud, Jr., Phys. Rev. A **14**, 1498 (1976).
[24] The blockade can be seen as an analog to the Autler-Townes splitting in the corresponding optical system.
[25] S. K. Dutta *et al.*, Phys. Rev. Lett. **86**, 3993 (2001).
[26] C. Ates *et al.*, Phys. Rev. Lett. **98**, 023002 (2007).
[27] T. G. Walker and M. Saffman, J. Phys. B **38**, S309 (2005).
[28] A. Reinhard *et al.*, Phys. Rev. A **75**, 032712 (2007).
[29] T. A. Johnson *et al.*, Phys. Rev. Lett. **100**, 113003 (2008).